Two-Step Linear Least-Squares Method for Photovoltaic Single-Diode Model Parameters Extraction

F. Javier Toledo, José M. Blanes and Vicente Galiano

***Abstract*— In this paper a new method to calculate the five parameters of the single-diode model of a photovoltaic cell or panel is presented. This new method takes into account the intrinsic properties of the model equation and the technique of linear least-squares fitting, so, the computational complexity and costs are very low. Moreover, the proposed method, named *Two-Step Linear Least-Squares* (*TSLLS*) method, is able to work absolutely blindly with any kind of *I-V* curve. It does not need initial guesses at all and, consequently, it is not necessary to know previously any information of any parameter. The proposed method provides the parameters of the single-diode model just using the coordinates of *N* points (*N≥5*) of the *I-V* curve. The results provided by this method in a first stage have the same order of accuracy of the best documented methods in the field of parameters extraction, but, furthermore, in a second stage the best accuracy documented until now is obtained in two important case studies usually used in the literature as well as in a large-scale *I-V* curve repository with more than one million of curves.**

***Index Terms*— Solar Cell Parameters; Characteristic *I-V* Curve; Single-Diode Model; Photovoltaic Energy.**

I. INTRODUCTION

DURING the last decades, the photovoltaic (*PV*) single-diode model has been one of the most used. It has been widely demonstrated that this model, also called five-parameter model, generates a theoretical curve that reproduces the real *I-V* characteristic of most of the *PV* cells and panels with very good accuracy under a minimum of illumination [1-3]. For this reason, researchers have attempted to extract the model parameters and companies have tried to use these parameters to deeply know the behavior of their *PV* cells or panels in order to optimize their performance. Furthermore, the knowledge of the model parameters has been also used for some new maximum power point tracking techniques (*MPPT*) [4,5]. For all these reasons, extraction of the model parameters is definitely a key tool in the field of solar energy production.

Many methodologies have been suggested in the literature for extraction of the model parameters. These methodologies can be divided into three groups: those that try to extract the parameters throughout the manufacturer datasheet [3, 6-12], those that attempt to obtain the parameters with a collection of experimental current-voltage points [13-28], and finally that ones that use both, the datasheet and also experimental data [29-31]. Among all these methods, there are some [11, 29] that extract the parameters as functions of the irradiance and the temperature. This allows, once the parameters are extracted, to extrapolate the parameters for different working conditions. It is worth noting that the method presented in this paper does obtain the parameters from a set of experimental current-voltage points but it does not provide any physical meaning of the parameters so, it must be executed every time environmental conditions change.

Recently, two papers, [21, 23], have provided the best solutions ever for two case studies proposed in [24] and also used in many papers [18-20, 25-28] to check the effectiveness of the proposed single-diode model extraction methods. Both papers, [21] and [23], use a common idea, suggested for the first time in [21], that consists in reducing the dimension of the parameter search space from 5 to 2 by expressing three of the parameters as a function of the other two. Specifically, [21] provides two reduced forms whose accuracy strongly depends of the precision of some needed operating data, namely, the short circuit current (I_{sc}), the open circuit voltage (V_{oc}), and the maximum power point (*MPP*). Moreover, the optimization process in [23] performs a least-squares fitting based in the two unknown parameters which clearly needs to start from a guess very near to the optimal solution to ensure, not only its convergence, but also a reduced number of iterations. In the case of [23], the method is based in

Manuscript received June 28, 2017; revised October 01, 2017; revised November 17, 2017; revised December 02, 2017; accepted December 20, 2017. This work was supported in part by Grant MTM2011-29064-C03-03 from MINECO, Spain, and Grant MTM2014-59179-C2-2-P from MINECO, Spain, and FEDER, European Union.

F. Javier Toledo is with the Center of Operations Research, University Miguel Hernández, 03202 Elche, Spain (phone: +34966658371 fax: +34966658715 e-mail: javier.toledo@umh.es).

José M. Blanes, is with the Industrial Electronics Group, University Miguel Hernández of Elche, 03202 Elche, Spain (e-mail: jmblanes@umh.es).

Vicente Galiano, is with the Physics and Computer Architecture Department, University Miguel Hernández of Elche, 03202 Elche, Spain (e-mail: vgaliano@umh.es).

performing an educated approximation of the original minimization problem depending on five parameters, then, through a generalized Benders-like decomposition, the problem is reduced to solve two problems in a nested form. After some approximations, they are able to provide a closed-form expression to express three parameters as a function of the other two. Finally, a least-squares fitting depending on the two unknown parameters is performed to obtain the optimal parameters but, as in the case of [21], it clearly needs to start from a guess very near to the optimal solution to ensure, not only its convergence, but also a reduced number of iterations. Although this last method does not depend on any operating data, I_{sc}, V_{oc}, and *MPP*, the approximations used in the construction of the method enclose some small deviations and induce some numerical problems that must be overcome with a casuistic procedure.

The method proposed in this paper, named *Two-Step Linear Least-Squares* (*TSLLS*) method, does not need any kind of extra information to work, just the coordinates of N points ($N \geq 5$) of the *I-V* curve and nothing else is required. The *TSLLS* method does not depend on the accuracy of any operating data, I_{sc}, V_{oc}, and *MPP*, and it does not need to know any good approximate solution of the parameters to use as initial guess. This method converges completely blindly to an optimal solution, which, in the case studies proposed in [24] has the same order of accuracy as the best documented provided by [21] and [23]. Besides, in a second stage, using the curve fitting technique, and only with the parameters obtained in the first stage as initial guess, it is obtained a slight improvement of the best results documented given in [21] and [23]. It is worth noting that the *TSLLS* method needs at least five points to work, so it cannot be applied if only datasheet information is available, experimental measurements are a must.

Finally, the methodology proposed in this paper allows to identify some properties of the *I-V* curves. Specifically, it is able to identify the most significant linear and exponential parts of the curve. These parts are closely related with the status of the *PV* panel and it could provide valuable information about the behavior of the panel in real conditions and also during the manufacturing process. It is worth mentioning that the *TSLLS* method works with almost any kind of *I-V* curve, even with those provided by panels with a large degradation.

The structure of the paper is as follows: In section II the theory of the *TSLLS* method and the procedure to extract the optimal parameters are presented. Experimental results of applying the *TSLLS* method to a solar cell and a solar panel commonly used in the literature and their comparison with some of the best parameters extraction methods is presented in section III. In section IV the experimental results coming from the application of the proposed method to a publicly repository of *I-V* curves is presented. Finally, section V presents the main conclusions of the work.

II. Two Step Linear Least-Squares Method

The single-diode model electrical circuit of a solar cell can be extrapolated to a *PV* module with n_p cells in parallel and n_s cells in series, see figure 1. At a given illumination, the relationship between the current and the voltage is given by the model equation (1):

$$I = n_p I_{ph} - n_p I_{sat}\left(e^{\frac{\frac{V}{n_s}+\frac{IR_s}{n_p}}{nV_T}} - 1\right) - n_p \frac{\frac{V}{n_s}+\frac{IR_s}{n_p}}{R_{sh}} \quad (1)$$

where I_{ph} is the photocurrent, I_{sat} is the diode saturation current, n is the diode ideality factor, $V_T=kT/q$, being T the temperature of the cell, k the Boltzmann's constant (*1.3806503E-23J/K*) and, q the electron charge (*1.602E-19C*), R_s is the series resistance of a cell and, R_{sh} is the shunt resistance of a cell.

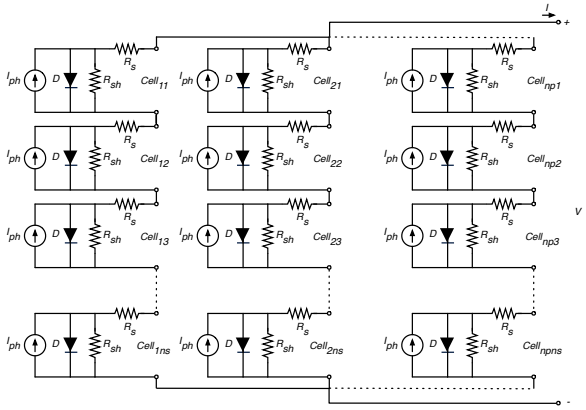

Fig. 1. PV Module single-diode model electrical circuit

Just making a simple change of variables (see, for instance, [16]), the *PV* model equation (1) can be rewritten in a simplified way as:

$$I = A - B(C^V D^I - 1) - EV \quad (2)$$

where

$$A = n_p I_{ph}\frac{R_{sh}}{R_{sh}+R_s},\ B = n_p I_{sat}\frac{R_{sh}}{R_{sh}+R_s},\ C = e^{\frac{1}{n_s nV_T}},$$
$$D = e^{\frac{R_s}{n_p nV_T}},\ E = \frac{n_p}{n_s}\frac{1}{R_{sh}+R_s} \quad (3)$$

The original parameters can be straightforwardly recovered from the new ones as:

$$I_{ph} = A\frac{1}{n_p}\frac{\ln(C)}{\ln(C)-E\ln(D)},\ I_{sat} = B\ \frac{1}{n_p}\frac{\ln(C)}{\ln(C)-E\ln(D)},$$
$$nV_T = \frac{1}{n_s}\frac{1}{\ln(C)},\ R_s = \frac{n_p}{n_s}\frac{\ln(D)}{\ln(C)},\ R_{sh} = \frac{n_p}{n_s}\left(\frac{1}{E} - \frac{\ln(D)}{\ln(C)}\right) \quad (4)$$

The model equation (2) can be rewritten as:

$$I = \underbrace{A + B - EV}_{linear\ part} - \underbrace{BC^V D^I}_{exponential\ part} \quad (5)$$

In (5), two very well distinguishable functional parts can be seen, a linear part $A + B - EV$, which corresponds with the oblique asymptote of the single-diode model [15], and an exponential part $BC^V D^I$. Obviously, these two parts are not independent of each other although their particular influence over the generated *I-V* curve can be easily perceived as figure 2 shows.

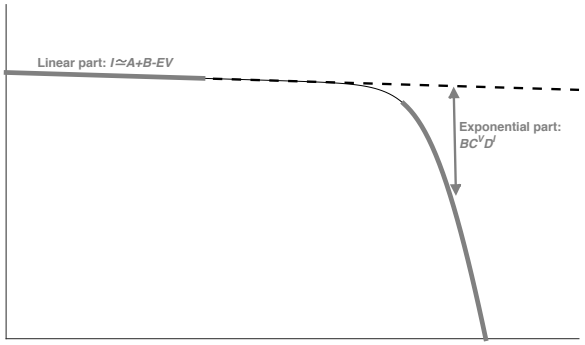

Fig. 2. Linear and exponential parts of the *I-V* Curve

TSLLS method tries to obtain separately, not independently, these two functional parts in a very simple way, although in a second stage it is optimized the identification of these two parts together with the extraction of the optimal parameters of the model. Let us assume we have a set of N points with coordinates (V_j, I_j), $j = 1, \dots, N$, from a given *I-V* curve. It is needed at least five points to apply the *TSLLS* method, that is, $N \geq 5$. As the name of the method indicates, it consists in the following two steps.

First Step

The linear part of the model equation is going to be extracted, that is, $A + B - EV$. It is assumed, without loss of generality, that the given *I-V* curve from the first point (V_1, I_1) (i.e. the point with the smallest voltage) to a certain point (V_L, I_L) is essentially a line, in other words, it is assumed that the exponential part $BC^V D^I$ is practically negligible in this first part of the curve and, so,

$$I \approx A + B - EV \tag{6}$$

The point $\left(V_{L_{op}}, I_{L_{op}}\right)$ that better determines the most significant linear part of the curve will be obtained a posteriori, when the optimal parameters are extracted. To start with the mathematical development, L points $(L \geq 2)$ of the given curve, $(V_1, I_1), \dots, (V_L, I_L)$, are selected. The objective is to find the line $I = K - EV$, where $K = A + B$, that best adjusts these points in the sense of least-squares errors. Specifically, it is wanted to obtain the least-squares solution (*K, E*) of the system (7)

$$\begin{bmatrix} 1 & -V_1 \\ \vdots & \vdots \\ 1 & -V_L \end{bmatrix} \begin{bmatrix} K \\ E \end{bmatrix} = \begin{bmatrix} I_1 \\ \vdots \\ I_L \end{bmatrix} \tag{7}$$

that is, the (pseudo-)solution with lowest Euclidean norm. It is well-known that this solution is given by

$$\begin{bmatrix} K \\ E \end{bmatrix} = \left(\Lambda_L^T \Lambda_L\right)^{-1} \Lambda_L^T \begin{bmatrix} I_1 \\ \vdots \\ I_L \end{bmatrix} \tag{8}$$

where

$$\Lambda_L = \begin{bmatrix} 1 & -V_1 \\ \vdots & \vdots \\ 1 & -V_L \end{bmatrix} \tag{9}$$

Λ_L^T is the transpose matrix of Λ_L, and $\left(\Lambda_L^T \Lambda_L\right)^{-1}$ is the inverse matrix of $\Lambda_L^T \Lambda_L$ which is a second order square matrix called the Moore-Penrose pseudoinverse of Λ_L. It is also well-known that the solution attained by this technique is unique when $rank(\Lambda_L) = 2$, which is indeed our case since $V_j \neq V_k$ for $j \neq k$. Observe that, this first step also reduces the dimension of the search space as in [21] and [23] but with other parameters and different methodology.

Second Step

Once the parameters $K = A + B$ and E have been obtained in the first step, the parameters B, C, and D of the exponential part can be extracted. The model equation (2) can be rewritten as:

$$BC^V D^I = K - EV - I \tag{10}$$

and, taking logarithms on the previous expression

$$\ln(B) + V\ln(C) + I\ln(D) = \ln\left(K - I - EV\right) \tag{11}$$

After this elementary algebraic manipulation, the desired parameters can be obtained throughout a linear least-squares fitting, but now, using M points $(M \geq 3)$ starting from the last one (V_N, I_N) to a certain (V_{N-M+1}, I_{N-M+1}). Now, the point $\left(V_{N-M_{op}+1}, I_{N-M_{op}+1}\right)$ that better determines the most significant exponential part of the curve will be obtained a posteriori, when the optimal parameters are extracted. It is important to mention that this point does not necessarily coincide with $\left(V_{L_{op}}, I_{L_{op}}\right)$.

The mathematical details of this second step are as follows. Select M points $(M \geq 3)$ of the given curve, $(V_{N-M+1}, I_{N-M+1}), \dots, (V_N, I_N)$. The parameters $\ln(B), \ln(C)$, and $\ln(D)$ which provide the best fitting of the function $\ln(B) + V\ln(C) + I\ln(D) = \ln\left(K - I - EV\right)$ over the selected points have to be obtained. Specifically, the (pseudo-) solution with minimum Euclidean norm of the system (12) has to be obtained.

$$\begin{bmatrix} 1 & V_{N-M+1} & I_{N-M+1} \\ \vdots & \vdots & \vdots \\ 1 & V_N & I_N \end{bmatrix} \begin{bmatrix} \ln(B) \\ \ln(C) \\ \ln(D) \end{bmatrix} = \begin{bmatrix} \ln(K - I_{N-M+1} - EV_{N-M+1}) \\ \vdots \\ \ln(K - I_N - EV_N) \end{bmatrix} \tag{12}$$

Analogously to Step 1, the least-squares solution for this system is given by (13):

$$\begin{bmatrix} \ln(B) \\ \ln(C) \\ \ln(D) \end{bmatrix} = \left(\Omega_M^T \Omega_M\right)^{-1} \Omega_M^T \begin{bmatrix} \ln\left(K - I_{N-M+1} - EV_{N-M+1}\right) \\ \vdots \\ \ln\left(K - I_N - EV_N\right) \end{bmatrix} \quad (13)$$

where

$$\Omega_M = \begin{bmatrix} 1 & V_{N-M+1} & I_{N-M+1} \\ \vdots & \vdots & \vdots \\ 1 & V_N & I_N \end{bmatrix} \quad (14)$$

Ω_M^T is the transpose matrix of Ω_M, and $\left(\Omega_M^T \Omega_M\right)^{-1}$ is the inverse matrix of $\Omega_M^T \Omega_M$ which is simply a square matrix of order 3. As commented before, the solution of the system is unique when $rank(\Omega_M) = 3$ which always occurs in practice because of the shape of the *I-V* curves. Obviously, the desired parameters B, C, and D straightforwardly come from taking exponentials on $\ln(B)$, $\ln(C)$, and $\ln(D)$, respectively, and finally $A = K - B$.

An immediate first approximation of the parameters can be obtained by a suitable selection of L points for the first step and M points for the second one, and it can be done just from a simple examination of the given curve, for instance, taking the first L points from the visual linear part of the curve, and the final M points from the elbow of the curve until the final. In this sense, the *TSLLS* method, until this stage, can be considered an analytical method since only with five data, in particular with only five points, provides the five parameters of the model. In the next stage, it is proposed a way to find the best data (in some sense) to apply this analytical method. Due to the simplicity of the previous two steps, the new stage can be programmed to work completely autonomously from a given set of *I-V* experimental points.

Blind Optimization Process

The optimization process consists on finding the subset of *I-V* experimental points that provides the parameters A, B, C, D, and E which minimizes the current *Root Mean Square Error* (*RMSE*) given by

$$RMSE = \sqrt{\frac{1}{N}\sum_{j=1}^{N}\left(I_j^P - I_j\right)^2} \quad (15)$$

where I_j is the measured current of the *PV* module, I_j^P is the estimated current from the method, for certain set of parameters $P = (A, B, C, D, E)$, corresponding to the voltage V_j, and N is the total number of available points. The minimum is searched between all the possible combinations of steps one and two described previously. This process is summarized in the algorithm shown in figure 3.

```
Set RMSE_opt = +∞
For L = 2 to N − 3
   Obtain K and E as in First Step (eq. 8)
   For M = 3 to L + 1
      Obtain B, C, D, and A as in Second Step (eq.13)
      Compute RMSE (eq. 15)
      If RMSE < RMSE_opt then
            RMSE_opt = RMSE
            P_opt = (A, B, C, D, E)
            N_opt = L and M_opt = M
      End
   End
```

Fig. 3 Blind Optimization Algorithm

Although the current *RMSE* is the most widely used in the literature, other objective functions to minimize could be also interesting to consider. For example, changing intensities by power in the *RMSE* equation [32, 33] can be very useful if the resolution of the model is used for *MPPT*. Nevertheless, there are lot of possibilities depending on the magnitude to minimize [14], some of them are voltages (lateral optimization), areas, distances, conductances, etc. The optimal solution will be different for each objective function and each one will be appropriate for a particular application.

The proposed optimization algorithm provides the parameters $P_{opt} = (A, B, C, D, E)$ associated to the *minimum Root Mean Square Error*, $RMSE_{opt}$, as well as the shape limit points, $\left(V_{N_{opt}}, I_{N_{opt}}\right)$ and $\left(V_{N-M_{opt}+1}, I_{N-M_{opt}+1}\right)$. These two points mark off on the curve the most significant linear part and the most significant exponential one.

It is important to note that, if the number of experimental points (*N*) is very high, a huge amount of iterations would be needed for this optimization process. In order to overcome this potential problem and to upper bound the number of iterations, the maximum number of points used in each curve has been set to 100, uniformly distributed in percentage of number of points. It has been experimentally proven that the difference between the accuracy obtained considering all the points or only taking 100 points is insignificant. So, if the curve has more than 100 points, it is reduced to 100 before the optimization process is applied. Therefore, since the number of iterations is $(N-3)\cdot(N-4)/2$, if $N \leq 100$ the maximum number of iterations is 4656.

The great advantage of the proposed method is to achieve the objective working completely blindly from the experimental data, so, this methodology can provide an optimal solution, near to the global one, just using experimental data and without any extra information.

Once obtained the optimal parameters in this first stage, it is possible to refine the solution by performing a curve fitting

with the experimental data, taking as starting point the parameters already obtained. This methodology is the same used in [21] and [23]. The success of this procedure will depend on whether the parameters of the first stage are close to the global optimum. This fitting is performed in *Matlab* using the function *lsqcurvefit* of the *Matlab Optimization Toolbox*. Due to the different order of magnitude of the involved parameters, the function *lsqcurvefit* does not directly provide the best possible solutions, but this issue can be overcome normalizing all the parameters (*A,B,C,D and E*) to 1 and, consequently, changing the objective function to accept the normalized parameters. The *Matlab* solver iterates to find an optimum (*steps*). At any step, intermediate calculation may involve evaluations of the objective function (*Function Evaluations (FEs)).* As the objective function in [21], [23] and in the proposed method is the same, the number of *steps* and *FEs* can be used to measure the computational cost of the *Matlab Optimization Toolbox* functions independently of the computer specifications.

III. Experimental results: Case Studies

With the aim to test the accuracy of the *TSLLS* method and to compare the results with other methods, two case studies commonly used in the literature have been modeled. These two cases were proposed in [24] and have been used in [17, 19-21, 23, 25-28] to test the corresponding proposed methods. It will be named *"Case Study 1"* the data (26 *I-V* points) provided in [24] referred to a solar module (*Photowatt-PWP 201*, 1000W/m^2, 45 °C) composed by 36 cells connected in series, and *"Case Study 2"* the data (26 *I-V* points) referred to a 57mm diameter silicon solar cell (*RTC France*, 1000W/m2, 33 °C). The *TSLLS* algorithm was implemented in *Matlab* and, from the first stage results, a refinement is performed using the fitting function *lsqcurvefit* of the Matlab *Optimization Toolbox*. As explained in [23], a lower value of *RMSE* (15) corresponds to a better fitting of the experimental data in terms of *Least-Squares Error* (*LSE*). In [21] it is already presented a comparison of all the results obtained in the literature for these case studies and in [23] it is only presented a comparison of their proposed method with the best documented until then that is [21]. In this paper, the *TSLLS* method results will be compared with the best accuracy methods documented up to now, that has been provided by [21] and [23]. Besides, since [21] performs a comparison with direct methods [27, 28] and different stochastic optimization methods [17, 19, 20, 26], the *TSLLS* method is actually being implicitly compared with all of them.

In the comparison, the results have been used as they appear in the mentioned articles [21] and [23], only the *RMSE* (15) and the *Mean Absolute Error* (*MAE)* (16) values have been recomputed in order to obtain a higher number of digits. To be fair in the comparison, the results of the *TSLLS* method have been truncated to the same number of digits presented in [21] and the *RMSE* and *MAE* values have been calculated with the truncated values.

$$MAE = \frac{1}{N}\sum_{j=1}^{N}\left|I_j^P - I_j\right| \quad (16)$$

Case Study 1 – PV Module

The parameters obtained are reported in *Table I*, the *RMSE* and the *MAE* values, the number of steps and the number of function evaluations (*FEs*). The solutions in the row named *TSLLS* are the ones obtained with the proposed method. The solutions in the row named *TSLLS with Refinement* are obtained doing a fitting of the data to minimize the *RMSE* over all the parameters near to the obtained by the *TSLLS* method. Both results are compared with the best documented in the literature. It is worth remarking that the *TSLLS* method is the only one that works completely blindly from the experimental data. The *RMSE* obtained by the *TSLLS* method before refinement is very low and has the same order of accuracy as the best documented. Furthermore, after the refinement, the *RMSE* obtained is the best documented until now and also the computational cost of the refinement is lower than in the other proposed methods since the algorithm converges in just 6 steps. It is important to highlight that, as in [21] and [23], these metrics only correspond to the refinement stage where an improvement of results is obtained by using the five parameters returned by a previous stage as initial guesses.

TABLE I
RESULTS FOR CASE STUDY 1 - PV MODULE (36 SOLAR CELLS, T=45°C)

	Laudani et al. Solution 1.D [21]	*Cardenas et al. Solution 1.b [23]*	*TSLLS*	*TSLLS With Refinement*
$I_{ph}(A)$	1.0323759	1.032377	1.0335685	1.0323823
$I_{sat}(\mu A)$	2.5188848	2.517957	2.2709763	2.5129059
$n_s{\cdot}R_s\,(\Omega)$	1.2390187	1.239060	1.2599674	1.3001512
$n_s{\cdot}R_{sh}\,(\Omega)$	745.6431	745.7122	687.87337	744.71302
n	1.3174002	1.3173635	1.3069558	1.3171591
RMSE	2.0465409E-3	2.0465456E-3	2.1722792E-3	**2.0465347E-3**
MAE	**1.6917202E-3**	1.6925284E-3	1.7242989E-3	1.6923215E-3
Number of steps	28	27	-	6
Number of FEs	204	141	-	42

It is also important to observe that all the methods compared try to minimize the *RMSE* not the *MAE*. The *RMSE* is minimized instead of the *MAE* error because in *RMSE* the errors are squared before they are averaged and this penalizes large errors in any point, what deals in a better fitting.

In figure 4, the upper graph shows the experimental data and the *I-V* curve modeled by the *TSLLS* method (without refinement). In this graph is also shown the optimal points (N_{opt} and M_{opt}) provided by the *TSLLS* method. The middle graph shows the error between all the 26 available experimental data points and the modeled points. As can be seen, the error is very low, less than 4.5mA in the worst case. The lower graph shows the same errors but after the refinement, it can be seen that the fitting in this case is slightly better with errors lower tan 4mA in the worst case. These results demonstrate that the assumption in [21] about the uniqueness of the solution attained is no longer true because the parameters obtained by the *TSLLS* method are different and provide a smaller *RMSE*.

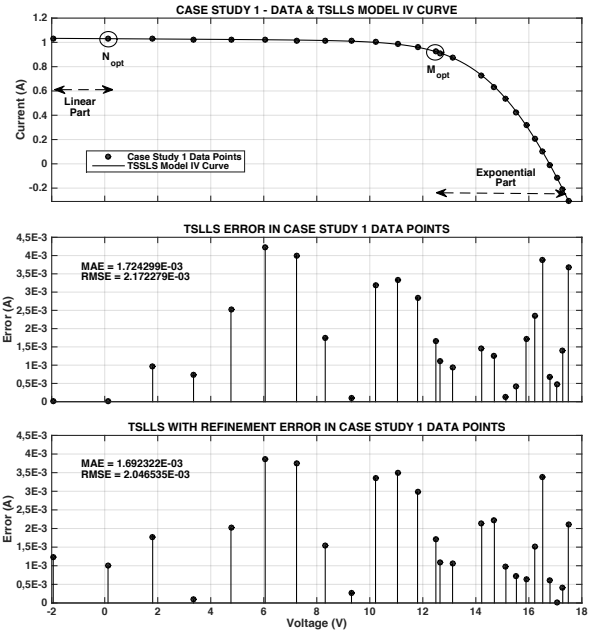

Fig. 4. Case Study 1 *TSLLS* Results

Case Study 2 – Solar Cell

The parameters obtained for the *Case Study 2* are reported in *Table II*, the nomenclature is the same used in *Table I*. The results show again that the *TSLLS* method has the best accuracy documented until now. The *RMSE* obtained by the *TSLLS* before refinement is very low and has the same order of accuracy as the best documented. After refinement, the *RMSE* obtained is again the best documented until now and the algorithm converges in just 3 steps.

In figure 5, the upper graph shows the experimental data and the *I-V* curve modeled by *TSLLS* method (without refinement). In this graph is also shown the optimal points (N_{opt} and M_{opt}) provided by the *TSLLS* method. The middle graph shows the error between all experimental data points and the model, in this case the error is less than 2mA in the worst case. The bottom graph shows the same errors but after the refinement with errors lower than 1.6mA in the worst case.

TABLE II
RESULTS FOR CASE STUDY 2 - SOLAR CELL (T=33°C)

	Laudani et al. Solution 1.D [21]	*Cardenas et al. Solution 1.b [23]*	*TSLLS*	*TSLLS With Refinement*
$I_{ph}(A)$	0.7607884	0.760788	0.76074014	0.76078797
$I_{sat}(\mu A)$	0.3102482	0.3106847	0.31285196	0.31068485
$R_s(\Omega)$	0.03655304	0.036547	0.036615485	0.036546942
$R_{sh}(\Omega)$	52.859056	52.890468	55.907380	52.889804
n	1.4769641	1.4771051	1.4777295	1.4771052
RMSE	7.73009395E-4	7.730062729E-4	7.943924087E-4	**7.730062726E-4**
MAE	6.7807111E-4	6.7817233E-4	**6.6795463E-4**	6.7819422E-4
Number of steps	16	8	-	3
Number of FEs	138	36	-	24

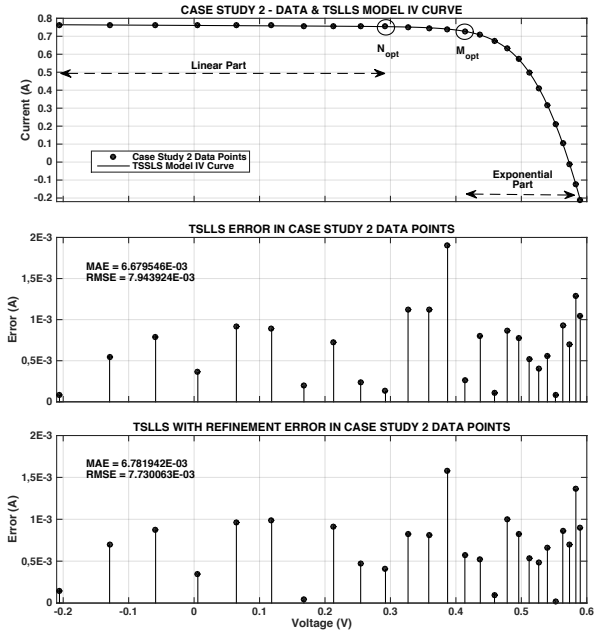

Fig. 5. Case Study 2 *TSLLS* Result

IV. EXPERIMENTAL RESULTS: NREL CURVE REPOSITORY

Once the accuracy of the *TSLLS* method has been demonstrated, the method has been applied to model a publicly repository of *I-V* curves available through the *National Renewable Energy Laboratory* (*NREL*) [34]. This repository includes 1025599 *I–V* curves from 22 *PV* modules, of eight different technologies, collected every five minutes for one year periods at three climatically diverse locations (Cocoa, Eugene and Golden). In order to apply the *TSLLS* method to these huge number of curves, the process has been automated with a python script running in a twenty-machines computer cluster. In *Table III* it is shown, for each different *PV* module and its location, the average *RMSE* and *MAE* obtained with the *TSLLS* method. Although the curves have been reduced to 100 points, to apply the blind optimization process the *RMSE* and *MAE* values have been computed using all the points of each curve. In *Table IV* the same values are shown but using the *TSLLS* method with refinement.

TABLE III
AVERAGE *RMSE* AND *MAE* OBTAINED WITH *TSLLS* METHOD

PV module - Location	*Curves*	$\overline{RMSE}$	$\overline{MAE}$
aSiMicro03036-Cocoa	*39037*	7.88E-04	6.46E-04
aSiMicro03036-Eugene	*43343*	7.14E-04	5.91E-04
aSiMicro03038-Golden	*12148*	4.40E-04	3.62E-04
aSiTandem72-46-Cocoa	*39186*	1.11E-03	9.62E-04
aSiTandem72-46-Eugene	*43266*	9.38E-04	8.08E-04
aSiTandem90-31-Golden	*12070*	1.59E-03	1.35E-03
aSiTriple28324-Cocoa	*38485*	3.92E-03	3.31E-03
aSiTriple28324-Eugene	*42705*	3.18E-03	2.67E-03
aSiTriple28325-Golden	*11445*	4.13E-03	3.47E-03
CdTe75638-Cocoa	*39080*	7.85E-03	6.62E-03
CdTe75638-Eugene	*42248*	6.86E-04	5.78E-04
CdTe75669-Golden	*11953*	9.98E-04	8.28E-04
CIGS8-001-Cocoa	*38939*	3.62E-03	3.10E-03
CIGS8-001-Eugene	*43146*	2.21E-03	1.90E-03
CIGS1-001-Golden	*12011*	2.21E-03	1.90E-03
CIGS39017-Cocoa	*34775*	6.52E-03	5.37E-03
CIGS39017-Eugene	*42674*	5.10E-03	4.30E-03
CIGS39013-Golden	*11437*	6.38E-03	5.37E-03
HIT05667-Cocoa	*38377*	3.60E-03	1.91E-03
HIT05667-Eugene	*43271*	6.41E-03	4.96E-03
HIT05662-Golden	*11876*	3.60E-03	1.91E-03
mSi0166-Cocoa	*36765*	2.37E-03	1.94E-03
mSi0166-Eugene	*43268*	1.92E-03	1.55E-03
mSi0247-Golden	*11912*	2.49E-03	2.08E-03
mSi0188-Cocoa	*39102*	1.83E-03	1.49E-03
mSi0188-Eugene	*43127*	1.54E-03	1.23E-03
mSi0251-Golden	*11887*	1.91E-03	1.57E-03
mSi460A8-Cocoa	*38929*	3.57E-03	2.58E-03
mSi460A8-Eugene	*43115*	2.30E-03	1.70E-03
mSi460BB-Golden	*11919*	8.90E-03	7.20E-03
xSi12922-Cocoa	*38989*	2.73E-03	2.06E-03
xSi12922-Eugene	*43185*	2.25E-03	1.72E-03
xSi11246-Golden	*11929*	2.29E-03	1.71E-03
AVERAGE	*31079*	3.07E-03	2.45E-03
MAXIMUM	*43343*	8.90E-03	7.20E-03

TABLE IV
AVERAGE *RMSE* AND *MAE* OBTAINED WITH *TSLLS* WITH REFINEMENT

PV module - Location	*Curves*	$\overline{RMSE}$	$\overline{MAE}$
aSiMicro03036-Cocoa	*39037*	2.81E-04	2.08E-04
aSiMicro03036-Eugene	*43343*	2.35E-04	1.60E-04
aSiMicro03038-Golden	*12148*	2.16E-04	1.79E-04
aSiTandem72-46-Cocoa	*39186*	1.01E-03	8.85E-04
aSiTandem72-46-Eugene	*43266*	8.36E-04	7.33E-04
aSiTandem90-31-Golden	*12070*	1.38E-03	1.20E-03
aSiTriple28324-Cocoa	*38485*	3.69E-03	3.14E-03
aSiTriple28324-Eugene	*42705*	2.97E-03	2.51E-03
aSiTriple28325-Golden	*11445*	3.79E-03	3.12E-03
CdTe75638-Cocoa	*39080*	7.34E-04	6.31E-04
CdTe75638-Eugene	*42248*	6.26E-04	5.39E-04
CdTe75669-Golden	*11953*	9.25E-04	7.84E-04
CIGS8-001-Cocoa	*38939*	3.01E-03	2.64E-03
CIGS8-001-Eugene	*43146*	2.87E-03	2.51E-03
CIGS1-001-Golden	*12011*	2.06E-03	1.79E-03
CIGS39017-Cocoa	*34775*	4.95E-03	4.01E-03
CIGS39017-Eugene	*42674*	3.67E-03	3.05E-03
CIGS39013-Golden	*11437*	4.17E-03	3.44E-03
HIT05667-Cocoa	*38377*	3.49E-03	1.83E-03
HIT05667-Eugene	*43271*	5.91E-03	4.96E-03
HIT05662-Golden	*11876*	3.49E-03	1.83E-03
mSi0166-Cocoa	*36765*	2.18E-03	1.82E-03
mSi0166-Eugene	*43268*	1.74E-03	1.43E-03
mSi0247-Golden	*11912*	2.30E-03	1.95E-03
mSi0188-Cocoa	*39102*	1.68E-03	1.39E-03
mSi0188-Eugene	*43127*	1.40E-03	1.14E-03
mSi0251-Golden	*11887*	1.72E-03	1.44E-03
mSi460A8-Cocoa	*38929*	2.83E-03	2.37E-03
mSi460A8-Eugene	*43115*	1.96E-03	1.62E-03
mSi460BB-Golden	*11919*	8.44E-03	7.19E-03
xSi12922-Cocoa	*38989*	2.36E-03	1.97E-03
xSi12922-Eugene	*43185*	2.04E-03	1.69E-03
xSi11246-Golden	*11929*	2.21E-03	1.57E-03
AVERAGE	*31079*	2.46E-03	1.99E-03
MAXIMUM	*43343*	8.44E-03	7.19E-03

These results include curves measured under partial shading conditions and also curves measured with low irradiance. In theory, these curves cannot be correctly modeled with the single-diode model. Nevertheless, the maximum *RMSE* error obtained for all the curves is 8.90E-03 without refinement and 8.44E-03 with refinement. The average *RMSE* and *MAE* values without refinement are 3.07E-03 and 2.45E-03 and with refinement 2.46E-03 and 1.99E-03. Compared with the results presented in [23] (*Average RMSE* 3.32E-03 and *Average MAE 2.68E-03,* both results with refinement), the results obtained with the *TSLLS* method (with and without refinement) are better. This is because in [23] the method needs initial guesses to work and, so, in order to process all the curves automatically without intervention, they had to fix the same initial guesses for all the curves of the repository. Nevertheless, the *TSLLS* method works absolutely blindly from the data. These results again demonstrate the accuracy and the robustness of the proposed method and its ability to work completely blindly.

It is worth noting that although, the single-diode model is valid at illuminations above one-half AM1 [2], using the *TSLLS* method curves at lower illuminations have been modeled with very low errors, but in this case the solution gives non-physical parameter values, like negatives series resistances.

V. CONCLUSIONS

In this paper, a new method to identify the five parameters of the single-diode model of a photovoltaic cell or panel is presented. This new method, named *TSLLS*, makes use of the specific geometrical properties of the *I-V* curve to directly extract the parameters from a set of *I-V* points. At least five points are needed to apply the method but, in general, more accurate results are obtained when more points are used. The great advantage of the *TSLLS* method, in comparison with other methods available in the literature, is its ability to work absolutely blindly. It does not need initial guesses at all and it is not necessary the knowledge of any information of any parameter (like *MPP*, I_{sc} or V_{oc}), for this reason it can be fully automated to work with any *I-V* curve.

The results provided by the *TSLLS* method have the same order of accuracy of the most accurate methods proposed in the literature, but, furthermore, in a second stage applying a refinement to the solutions obtained by the *TSLLS* method, the best accuracy documented until now in the literature has been obtained in two important case studies usually used in the literature.

The potential of the *TSLLS* method has been also demonstrated modeling 1025599 *I-V* curves from the *NREL*

repository with the best precision documented until now and working completely blindly from the data.

In order that any interested researchers can test the *TSLLS* method with their own curves, a webpage has been developed (*pvmodel.umh.es*) where the method can be directly tested online.

ACKNOWLEDGMENT

Authors would like to thank the *National Renewable Energy Laboratory* (*NREL*) for providing some of the *I-V* curves used in this research.

REFERENCES

[1] J. Charles, M. Abdelkrim, Y. Muoy and P. Mialhe, "A practical method of analysis of the current voltage characteristics of solar cells," Sol. Cells, vol. 4, pp. 169-178, 1981.
[2] D. Chan, J. Philips and J. Phang, "A comparative study of extraction methods for solar cell model parameters," Solid-St. Electron, vol. 29, no. 3, pp. 329-337, 1986.
[3] W. De Soto, S. Klein and W. Beckman, "Improvement and validation of 273 a model for photovoltaic array performance," Solar Energy, vol. 80, no. 1, pp. 78-88, 2006.
[4] M. Jedari Zare Zadeh and S. H. Fathi, "A New Approach for Photovoltaic Arrays Modeling and Maximum Power Point Estimation in Real Operating Conditions," in IEEE Transactions on Industrial Electronics, vol. 64, no. 12, pp. 9334-9343, Dec. 2017.
[5] J. S. C. M. Raj and A. E. Jeyakumar, "A Novel Maximum Power Point Tracking Technique for Photovoltaic Module Based on Power Plane Analysis of I–V Characteristics," in IEEE Transactions on Industrial Electronics, vol. 61, no. 9, pp. 4734-4745, Sept. 2014.
[6] A. Laudani, F. Riganti-Fulginei, A. Salvini and F. Mancilla-David, "Reduced-form of the photovoltaic five-parameter model for efficient computation of parameters," Sol. Energy, vol. 97, pp. 122-127, 2013.
[7] Y. Mahmoud, W. Xiao and H. Zeineldin, "A parameterization approach for enhancing PV model accuracy," IEEE Trans. Ind. Electron., vol. 60, no. 12, pp. 5708-5716, 2013.
[8] A. Orioli and A. Gangi, "A procedure to calculate the five-parameter model of crystalline silicon photovoltaic modules on the basis of the tabular performance data," Appl. Energy, vol. 102, pp. 1160-1177, 2013.
[9] A. Laudani, F. Riganti-Fulginei and A. Salvini, "Identification of the one-diode model for photovoltaic modules from datasheet values," Solar Energy, vol. 108, pp. 432-446, 2014.
[10] Y. Mahmoud and E. F. El-Saadany, "A Photovoltaic Model With Reduced Computational Time," in IEEE Transactions on Industrial Electronics, vol. 62, no. 6, pp. 3534-3544, June 2015.
[11] V. J. Chin, Z. Salam and K. Ishaque, "An Accurate and Fast Computational Algorithm for the Two-diode Model of PV Module Based on a Hybrid Method," in IEEE Transactions on Industrial Electronics, vol. 64, no. 8, pp. 6212-6222, Aug. 2017.
[12] J. J. Soon and K. S. Low, "Optimizing Photovoltaic Model for Different Cell Technologies Using a Generalized Multidimension Diode Model," in IEEE Transactions on Industrial Electronics, vol. 62, no. 10, pp. 6371-6380, Oct. 2015.
[13] F. Toledo, J. Blanes, A. Garrigós and J. Martínez, "Analytical resolution of the electrical four-parameters model of a photovoltaic module using small perturbation around the operating point," Renew. Energ., vol. 43, pp. 83-89, 2012.
[14] J. Blanes, F. Toledo, S. Montero and A. Garrigós, "In-Site Real-Time Photovoltaic I-V Curves and Maximum Power Point Estimator," IEEE Trans. Power Electr., vol. 28, pp. 1234-1240, 2013.
[15] F. Toledo and J. Blanes, "Geometric properties of the single-diode photovoltaic model and a new very simple method for parameters extraction," Renewable Energy, vol. 72, pp. 125-133, 2014.
[16] F. Toledo and J. Blanes, "Analytical and quasi-explicit four arbitrary point method for extraction of solar cell single-diode model parameters," Renewable Energy, vol. 92, pp. 346-356, 2016.
[17] M. AlHajri, K. El-Naggar, M. AlRashidi and A. Al-Othman, "Optimal extraction of solar cell parameters using pattern search," Renew. Energy, vol. 44, pp. 238-245, 2012.
[18] A. Askarzadeh and A. Rezazadeh, "Parameter identification for solar cell models using harmony search-based algorithms," Solar Energy, vol. 86, no. 11, pp. 3241-3249, 2012.
[19] K. El-Naggar, M. AlRashidi, M. AlHajri and A. Al-Othman, "Simulated annealing algorithm for photovoltaic parameters identification," Solar Energy, vol. 86, no. 1, pp. 266-274, 2012.
[20] L. Jiang, D. Maskell and J. Patra, "Parameter estimation of solar cells and modules using an improved adaptive differential evolution algorithm," Appl. Energy, vol. 112, pp. 185-193, 2013.
[21] A. Laudani, F. Riganti-Fulginei and A. Salvini, "High performing extraction procedure for the one–diode model of a photovoltaic panel from experimental I–V curves by using reduced forms," Solar Energy, vol. 103, pp. 316-326, 2014.
[22] L. Lim, Z. Z. Ye, J. Ye, D. Yang and H. Du, "A linear identification of diode models from single IV characteristics of PV panels," IEEE Trans.Ind. Electron., vol. 62, no. 7, pp. 4181-4193, 2015.
[23] A. Cárdenas, M. Carrasco, F. Mancilla-David, A. Street and R. Cárdenas, "Experimental Parameter Extraction in the Single-Diode Photovoltaic Model via a Reduced-Space Search," IEEE Trans. Ind. Electron., vol. 64, no. 2, pp. 1468-1476, 2017.
[24] T. Easwarkhanthan, J. Bottin, I. Bouhouch and C. Boutrit, "Nonlinear minimization algorithm for determining the solar cell parameters with microcomputers," Int. J. Sol. Energy, vol. 4, pp. 1-12, 1986.
[25] M. AlRashidi, M. AlHajri, K. El-Naggar and A. Al-Othman, "A new estimation approach for determining the IV characteristics of solar cells," Sol. Energy, vol. 85, pp. 1543-1550, 2011.
[26] W. Gong and Z. Cai, "Parameter extraction of solar cell models using repaired adaptive differential evolution," Sol. Energy, vol. 94, pp. 209-220, 2013.
[27] L. Peng, Y. Sun, Z. Meng, Y. Wang and Y. Xu, "A new method for determining the characteristics of solar cells," J.Power Sources, vol. 227, pp. 131-136, 2013.
[28] J. Cubas, S. Pindado and M. Victoria, "On the analytical approach for modeling photovoltaic systems behavior," J. Power Sources, vol. 247, pp. 467-474, 2014.
[29] S. Lineykin, M. Averbukh and A. Kuperman, "Issues in Modeling Amorphous Silicon Photovoltaic Modules by Single-Diode Equivalent Circuit," in IEEE Transactions on Industrial Electronics, vol. 61, no. 12, pp. 6785-6793, Dec. 2014.
[30] P. H. Huang, W. Xiao, J. C. H. Peng and J. L. Kirtley, "Comprehensive Parameterization of Solar Cell: Improved Accuracy With Simulation Efficiency," in IEEE Transactions on Industrial Electronics, vol. 63, no. 3, pp. 1549-1560, March 2016.
[31] J. D. Bastidas-Rodríguez, E. Franco, G. Petrone, C. A. Ramos-Paja and G. Spagnuolo, "Model-Based Degradation Analysis of Photovoltaic Modules Through Series Resistance Estimation," in IEEE Transactions on Industrial Electronics, vol. 62, no. 11, pp. 7256-7265, Nov. 2015.
[32] E. A. Silva, F. Bradaschia, M. C. Cavalcanti and A. J. Nascimento, "Parameter Estimation Method to Improve the Accuracy of Photovoltaic Electrical Model," in IEEE Journal of Photovoltaics, vol. 6, no. 1, pp. 278-285, Jan. 2016.
[33] W. Luo et al., "In-Situ Characterization of Potential-Induced Degradation in Crystalline Silicon Photovoltaic Modules Through Dark I–V Measurements," in IEEE Journal of Photovoltaics, vol. 7, no. 1, pp. 104-109, Jan. 2017.
[34] B. Marion et al, "New data set for validating PV module performance models," in 2014 IEEE 40th Photovoltaic Specialist Conference (PVSC), Denver, 2014.

F. Javier Toledo was born in Almoines, Spain, in 1973. He received the M.Sc. degree in mathematics from the University of Valencia, Spain, in 1997, and the Ph.D. degree from the Miguel Hernández University of Elche (UMH), Spain, in 2003.
He is currently an Associate Professor in the Department of Statistics, Mathematics and Informatics, UMH, and a Researcher in the Institute "Center of Operations Research" (CIO), UMH. His research interests are divided into two lines, stability in optimization in the field of mathematics and photovoltaics in the field of engineering.

José M. Blanes was born in Elche, Spain, in 1974. He received the M.Sc. degree on telecommunication engineering from the Universidad Politécnica de Valencia in 1998 and the Ph.D. degree on industrial technologies from the University Miguel Hernández de Elche in 2011.

He is currently an Associate Professor in the Materials Science, Optics and Electronics Technology Department of the University Miguel Hernandez of Elche, Spain. His main research areas are space power systems and industrial electronics.

Vicente Galiano is an Associate Professor in the Physics and Computer Architecture Department at the Miguel Hernandez University in Elche (Spain). He received the M.Sc degree in telecommunication engineering from the Polytechnic University of Valencia, and the Ph.D. degree in computer science in 2007 from the University Miguel Hernandez. His main research interests include high level interfaces design in parallel libraries and parallel simulations for modeling electronic systems.